

## Approximate Motion Planning and the Complexity of the Boundary of the Union of Simple Geometric Figures<sup>1</sup>

Helmut Alt,<sup>2</sup> Rudolf Fleischer,<sup>3</sup> Michael Kaufmann,<sup>3</sup>  
Kurt Mehlhorn,<sup>3</sup> Stefan Näher,<sup>3</sup> Stefan Schirra,<sup>3</sup>  
and Christian Uhrig<sup>3</sup>

**Abstract.** We study rigid motions of a rectangle amidst polygonal obstacles. The best known algorithms for this problem have a running time of  $\Omega(n^2)$ , where  $n$  is the number of obstacle corners. We introduce the *tightness* of a motion-planning problem as a measure of the difficulty of a planning problem in an intuitive sense and describe an algorithm with a running time of  $O((a/b \cdot 1/\varepsilon_{\text{crit}} + 1)n(\log n)^2)$ , where  $a \geq b$  are the lengths of the sides of a rectangle and  $\varepsilon_{\text{crit}}$  is the tightness of the problem. We show further that the complexity (= number of vertices) of the boundary of  $n$  bow ties (see Figure 1) is  $O(n)$ . Similar results for the union of other simple geometric figures such as triangles and wedges are also presented.

**Key Words.** Computational geometry, Motion planning, Boundary complexity, Combinatorial geometry, Analysis of algorithms.

**1. Introduction.** We consider the motion planning problem for a rectangle in the plane amidst polygonal obstacles. Such a problem is specified by a set of polygons with a total of  $n$  corners, the obstacles, a rectangle  $R$  with sides  $a$  and  $b$ ,  $a \geq b$ , and an initial and a final placement  $Z_1$  and  $Z_2$  of  $R$ . A placement  $Z = (x, y, \alpha)$  specifies the coordinates  $(x, y)$  of the center of  $R$  and the angle  $\alpha$  between the  $a$ -side of  $R$  and the positive  $x$ -axis. The question is to decide whether there is a rigid motion which moves  $R$  from  $Z_1$  to  $Z_2$  and avoids all the obstacles.

The best known algorithms for this problem have running times of  $O(n\lambda_3(n) \log n)$  [CK] and  $O(n\lambda_6(n) \log n)$  [KS2] respectively, where  $\lambda_s(r)$  is the maximum length of an  $(r, s)$ -Davenport–Schinzel sequence [S]. This is  $\Omega(n^2)$  and hence the algorithms are not feasible for large  $n$ .

<sup>1</sup> This work was supported partially by the DFG Schwerpunkt Datenstrukturen und Algorithmen, Grants Me 620/6 and Al 253/1, and by the ESPRIT II Basic Research Actions Program of the EC under Contract No. 3075 (project ALCOM).

<sup>2</sup> Fachbereich Mathematik, Freie Universität Berlin, Arnimallee 2-6, 1000 Berlin 33, Federal Republic of Germany.

<sup>3</sup> Max-Planck-Institut für Informatik, Im Stadtwald, W-6600 Saarbrücken, Federal Republic of Germany.

It is customary to measure the performance of motion planning algorithms as a function of the problem size, here, the number of corners of polygonal obstacles. However, problem size captures only part of the intuitive notion of difficulty of a planning problem. Another crucial parameter is the tightness of the problem, i.e., how small a change in the input changes the state of the problem from solvable to unsolvable and vice versa. We propose the following definition of tightness:

DEFINITION. Let  $\mathcal{P} = (P, R, Z_1, Z_2)$  be a motion planning problem. For real number  $\alpha > 0$  we use  $\alpha R$  to denote the rectangle with sides  $\alpha a$  and  $\alpha b$  and  $\mathcal{P}_\alpha$  to denote the problem  $(P, \alpha R, Z_1, Z_2)$ . The *tightness*  $\varepsilon_{\text{crit}}$  of  $\mathcal{P}$  is now given as follows:

- (a) If  $\mathcal{P}$  is solvable, then  $\varepsilon_{\text{crit}} = \inf\{\varepsilon; \mathcal{P}_{1+\varepsilon} \text{ is unsolvable}\}$ .
- (b) If  $\mathcal{P}$  is unsolvable, then  $\varepsilon_{\text{crit}} = \inf\{\varepsilon; \mathcal{P}_{1/(1+\varepsilon)} \text{ is solvable}\}$ .

We show:

THEOREM 1. *The motion planning problem for a rectangle amidst polygonal obstacles can be solved in time  $O(((a/b)(1/\varepsilon_{\text{crit}}) + 1)n(\log n)^2)$ , where  $n$  is the number of corners of the polygons,  $\varepsilon_{\text{crit}}$  is the tightness of the problem, and  $a \geq b$  are the lengths of the sides of the rectangle.*

The running time of our algorithm depends on the tightness of the problem. In particular, “easy” problems with  $\varepsilon_{\text{crit}} \geq \varepsilon_0$  for a fixed  $\varepsilon_0 > 0$  and  $a/b \leq k$  for some fixed  $k$  can be solved in time  $O(n(\log n)^2)$ . This is feasible even for large  $n$ . “Difficult” problems with either  $\varepsilon_{\text{crit}}$  close to zero or  $a/b$  very large take longer.

Our results can also be phrased as follows. Let  $\varepsilon > 0$  be fixed. An algorithm for the motion planning problem is said to be  $\varepsilon$ -approximate if it has the following property: If the algorithm declares a problem  $\mathcal{P}$  solvable, then the problem is indeed solvable. If the algorithm declares a problem unsolvable, then the problem  $\mathcal{P}_{1+\varepsilon}$  must indeed be unsolvable. Note that the answers of an  $\varepsilon$ -approximate algorithm are not completely reliable; there is a margin of error determined by the parameter  $\varepsilon$ .

THEOREM 2. *For all  $\varepsilon$ ,  $0 < \varepsilon \leq \sqrt{1 + a^2/b^2} - 1$ , there is an  $\varepsilon$ -approximate algorithm for moving a rectangle amidst polygonal obstacles with running time  $O((a/b)(1/\varepsilon)n(\log n)^2)$ .* -

The idea underlying the theorems is simple and by no means new; it was used in [LPW] to derive motion-planning heuristics. However, our analysis has some novel features. We discretize rotations and consider only so-called  $\theta$ -motions, where  $\theta$  is a fixed rotation angle. Let  $L = \{\alpha_1, \alpha_2\} \cup \{i\theta; i = 0, \dots, \lfloor 2\pi/\theta \rfloor\}$ , where  $\alpha_1$  and  $\alpha_2$  are the orientations in the initial and final placement, respectively. A  $\theta$ -motion consists of a sequence of steps. In each step the rectangle is either rotated about its center from one orientation in  $L$  to an adjacent one or it is translated. During translation the orientation of the rectangle is kept fixed to an orientation in  $L$ .

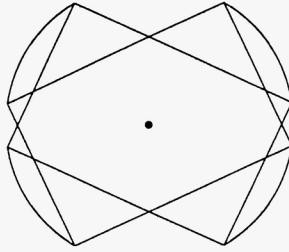


Fig. 1.

Translational movement of a rectangle is a well-studied topic. In [KS1] and [KLPS] an  $O(n(\log n)^2)$  algorithm and in [LeS] an  $O(n \log n)$  algorithm for this problem were given. We use the former algorithm as a subroutine in our algorithm.

An essential technical contribution of this paper is a detailed study of rotational movement in  $\theta$ -motions of a rectangle amidst point obstacles. Assume that  $R$ 's  $a$ -side is parallel to the  $x$ -axis and consider the figure swept out by  $R$  by rotating it from  $-\theta/2$  to  $\theta/2$  about its center, see Figure 1. Each obstacle point defines a forbidden region of just this shape. We show that free space (= complement of the union of the forbidden regions) consists of  $O(n)$  connected components and that the total number of vertices on the boundary of free space is also  $O(n)$ .

Using this complexity result we show

**THEOREM 3.** *The existence of a  $\theta$ -motion amidst  $n$  point obstacles can be decided in time  $O((1/\theta) n (\log n)^2)$ , if  $\theta \leq 2 \arctan(b/a)$ , where  $a \geq b$  are the lengths of the sides of the rectangle.*

We also show complexity bounds for the free space defined by other simple geometric figures, e.g., wedges and triangles, which we believe to be of independent interest. Our bounds on the complexity of free space are based on geometric and topological reasoning. In contrast, the linear bound for the complexity of the boundary of a union of circles can be obtained by purely topological reasoning [LiS], [KLPS].

The paper is organized as follows. In Section 2 we prove Theorems 1 and 2. Moreover, we prove Theorem 3 using the complexity bounds for free space derived in Section 3. Section 4 offers a conclusion and some open problems.

**2. The Algorithm.** In this section we give some further definitions, prove Theorems 1–3, and connect them to the results of Section 3.

**LEMMA 2.1.** *Theorem 2 implies Theorem 1.*

**PROOF.** Let  $A_\varepsilon$  be an  $\varepsilon$ -approximate algorithm with running time  $O((a/b)(1/\varepsilon)n(\log n)^2)$ .  $A_\varepsilon$  exists for  $0 < \varepsilon \leq \sqrt{1 + a^2/b^2} - 1$  by Theorem 2. Consider the following algorithm:

```

 $\varepsilon \leftarrow \sqrt{1 + a^2/b^2} - 1;$ 
while  $A_\varepsilon$  declares  $\mathcal{P}$  unsolvable and  $A_\varepsilon$  declares  $\mathcal{P}_{1/(1+\varepsilon)}$  solvable do
     $\varepsilon \leftarrow \varepsilon/2$  od
if  $A_\varepsilon$  declares  $\mathcal{P}$  solvable
    then return “solvable”
    else return “unsolvable”
fi
    
```

The correctness of this algorithm is easy to see. When the algorithm terminates either  $A_\varepsilon$  declares  $\mathcal{P}$  solvable or  $A_\varepsilon$  declares  $\mathcal{P}_{1/(1+\varepsilon)}$  unsolvable. In the former case,  $\mathcal{P}$  is indeed solvable. In the latter case,  $\mathcal{P} = (\mathcal{P}_{1/(1+\varepsilon)})_{1+\varepsilon}$  is indeed unsolvable. The running time of the algorithm is  $O((a/b)(1/\varepsilon_0)n(\log n)^2)$ , where  $\varepsilon_0$  is the final value of  $\varepsilon$ . It remains to relate  $\varepsilon_0$  and  $\varepsilon_{\text{crit}}$ . Consider an iteration which is not the last. Then  $A_\varepsilon$  declares  $\mathcal{P}$  unsolvable and hence  $\mathcal{P}_{1+\varepsilon}$  is indeed unsolvable, and  $A_\varepsilon$  declares  $\mathcal{P}_{1/(1+\varepsilon)}$  solvable. If  $\mathcal{P}$  is solvable, then  $\varepsilon_{\text{crit}} \leq \varepsilon$  by the unsolvability of  $\mathcal{P}_{1+\varepsilon}$ , and if  $\mathcal{P}$  is unsolvable, then  $1/(1 + \varepsilon_{\text{crit}}) \geq 1/(1 + \varepsilon)$  by the solvability of  $\mathcal{P}_{1/(1+\varepsilon)}$ . Thus  $\varepsilon_{\text{crit}} \leq \varepsilon$  in either case. This implies that either  $\varepsilon_0 = \sqrt{1 + a^2/b^2} - 1$  or  $\varepsilon_{\text{crit}} \leq 2\varepsilon_0$ . Hence the running time is within  $O(((a/b)(1/\varepsilon_{\text{crit}}) + 1)n(\log n)^2)$ .  $\square$

We next turn to the proof of Theorem 2. Consider the following algorithm:

*Input:*  $\mathcal{P} = (P, R, Z_1, Z_2)$  with  $Z_i = (x_i, y_i, \alpha_i)$  and  $\varepsilon > 0$ .

```

    Let  $\theta = 2 \min((b/a)\varepsilon, \pi/2 - \arctan(b/a));$ 
    if a  $\theta$ -motion exists for  $\mathcal{P}$ 
        then declare  $\mathcal{P}$  solvable
        else declare  $\mathcal{P}$  unsolvable fi
    
```

**LEMMA 2.2.** *The above algorithm is  $\varepsilon$ -approximate.*

**PROOF.** We only have to show that if  $\mathcal{P}$  does not allow a  $\theta$ -motion, then  $\mathcal{P}_{1+\varepsilon}$  does not allow any motion. It is easier to show the contrapositive, i.e., if  $\mathcal{P}_{1+\varepsilon}$  has a solution, then  $\mathcal{P}$  allows a  $\theta$ -motion. The following claim is helpful.

**CLAIM.** *A rectangle  $R$  with sides  $a$  and  $b$ ,  $a \geq b$ , can be rotated by  $\theta/2$  degrees in both directions within the rectangle  $(1 + \varepsilon)R$  if*

$$\varepsilon \geq \frac{a}{b} \sin\left(\frac{\theta}{2}\right) - 2 \sin^2\left(\frac{\theta}{4}\right) \quad \text{and} \quad \theta \leq \pi - 2 \arctan\left(\frac{b}{a}\right).$$

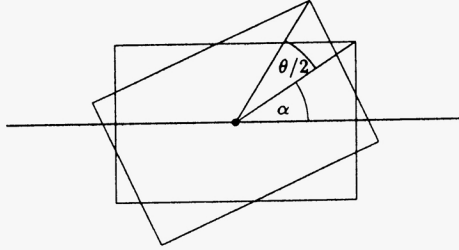


Fig. 2.

Both conditions hold true for

$$\theta = 2 \min\left(\frac{b}{a} \varepsilon, \frac{\pi}{2} - \arctan\left(\frac{b}{a}\right)\right).$$

PROOF. Let  $\alpha = \arctan(b/a)$  and  $d = \sqrt{a^2 + b^2}/2$ . Rotate  $R$  by  $\theta/2$  degrees, see Figure 2. Let  $R'$  be the figure obtained. Then the maximal  $x$ -coordinate of any point of  $R'$  is  $d \cos(\alpha - \theta/2)$  if  $\theta \leq 2\alpha$  (resp.  $d$  if  $\theta \geq 2\alpha$ ) and the maximal  $y$ -coordinate of any point of  $R'$  is  $d \sin(\alpha + \theta/2)$ . Hence  $R$  can be rotated by  $\theta/2$  degrees within  $(1 + \varepsilon)R$  provided that

$$1 + \varepsilon \geq \max\left(\frac{d \cos(\max(0, \alpha - \theta/2))}{a/2}, \frac{d \sin(\alpha + \theta/2)}{b/2}\right).$$

A short calculation shows that this is equivalent to

$$1 + \varepsilon \geq \cos\left(\frac{\theta}{2}\right) + \frac{a}{b} \sin\left(\frac{\theta}{2}\right) \quad \text{or} \quad \varepsilon \geq \frac{a}{b} \sin\left(\frac{\theta}{2}\right) - 2 \sin^2\left(\frac{\theta}{4}\right).$$

Note that the rotation figure is the disk with radius  $d$  if  $\theta \geq \pi - 2 \arctan(b/a)$ . Finally, observe that  $\theta \leq 2(b/a)\varepsilon$  implies  $(a/b) \sin(\theta/2) \leq \varepsilon$ . □

Assume now that there is a motion for rectangle  $(1 + \varepsilon)R$ . We will construct a  $\theta$ -motion from it. A placement of  $(1 + \varepsilon)R$  is given by the coordinates  $(x, y)$  of the center and the orientation  $\varphi$ . A corresponding placement of  $R$  is  $(x, y, \hat{\varphi})$  where  $\hat{\varphi} \in L = \{\alpha_1, \alpha_2, i\theta; i = 0, \dots, \lfloor 2\pi/\theta \rfloor\}$  and  $|\varphi - \hat{\varphi}|$  is minimal. Then  $|\varphi - \hat{\varphi}| \leq \theta/2$ . Also whenever  $\hat{\varphi}$  changes, the translational movement of  $R$  is stopped and  $R$  is turned into an adjacent orientation in  $L$ . The motion obtained is clearly a  $\theta$ -motion. It avoids all obstacles as can be seen as follows. Consider a coordinate system whose origin is the center of  $(1 + \varepsilon)R$  and whose  $x$ -axis is parallel to the  $a$ -side of  $(1 + \varepsilon)R$ , i.e., the system moves with  $(1 + \varepsilon)R$ . In this system the coordinates of  $R$  are  $(0, 0, \varphi')$  where  $|\varphi'| \leq \theta/2$  by the construction of  $R$ 's motion and hence  $R$  is always contained within  $(1 + \varepsilon)R$  by the claim above. □

We discuss next how to decide the existence of a  $\theta$ -motion. Let  $L = \{\theta_0, \dots, \theta_{l-1}\}$ , where  $l \leq 2 + 2\pi/\theta$ , be the set of allowed orientations with  $\theta_0 < \theta_1 < \dots < \theta_{l-1}$ .

A placement  $(x, y, \alpha)$  of  $R$  is *free (semifree)* if the rectangle does not contain any obstacle point (in its interior). Let  $FP$  denote the set of free placements. A general motion from placement  $Z_1$  to placement  $Z_2$  is possible iff  $Z_1$  and  $Z_2$  belong to the same connected component of  $FP$ . Let  $FP_\beta$  be the set of free placements of  $R$  in orientation  $\beta$ , i.e., the intersection of  $FP$  with  $\alpha = \beta$ . We identify  $FP_\beta$  with its projection on the  $xy$ -plane. Furthermore, let  $FP_{\theta_r, \theta_s}$  be the set of placements of the center of  $R$ , where  $R$  can be rotated from orientation  $\theta_r$  to orientation  $\theta_s$  without collision with the obstacle polygons.  $FP_{\theta_r, \theta_s}$  is the set of free placements of the rotation figure  $R_{\theta_r, \theta_s}$ , which is the set of points covered by the rectangle during the rotation.

Following the classical approach we reduce the decision problem to a search problem on an undirected graph  $G = (\bigcup_{i=0}^{l-1} V_i, E)$ . Each vertex of  $V_i$  represents a connected component of  $FP_{\theta_i}$ . Let  $C_u$  be the connected component of  $FP_{\theta_i}$  represented by  $u \in V_i$ . There is an edge connecting  $u \in V_i$  and  $v \in V_{i+1}$  iff  $C_u \cap C_v \cap FP_{\theta_i, \theta_{i+1}} \neq \emptyset$ . Clearly, there is a  $\theta$ -motion of  $R$  from placement  $Z_1$  with orientation  $\theta_{k_1}$  to placement  $Z_2$  with orientation  $\theta_{k_2}$  iff there is a path in  $G$  from the vertex in  $V_{k_1}$  representing the connected component that contains  $Z_1$  to the vertex in  $V_{k_2}$  representing the connected component that contains  $Z_2$ .

For the design of an  $\varepsilon$ -approximate algorithm it is sufficient to consider *restricted  $\theta$ -motions*: rotation is allowed only if the smallest rectangle similar to  $R$  that contains the rotation figure of  $R$  can be placed at the rotation point without collision with the obstacle polygons. Hence instead of  $FP_{\theta_i, \theta_{i+1}}$  we consider free space  $FP'_{\theta_i, \theta_{i+1}}$  of  $(1 + \varepsilon)R$  in orientation  $(\theta_i + \theta_{i+1})/2$ , where

$$\varepsilon = \frac{a}{b} \sin\left(\frac{\theta}{2}\right) - 2 \sin^2\left(\frac{\theta}{4}\right).$$

By the same argumentation as in Lemma 2.2 such a restricted  $\theta$ -motion exists, whenever a motion for  $(1 + \varepsilon)R$  exists.

We also change our definition of  $G$  slightly. There is an edge connecting  $u \in V_i$  and  $v \in V_{i+1}$  iff  $C_u \cap C_v \cap FP'_{\theta_i, \theta_{i+1}} \neq \emptyset$ . Let  $E'$  be the set of such edges. The graph  $G' = (V = \bigcup V_i, E')$  can be obtained as follows. It is well known that the complexity of  $FP_\theta$ , i.e., the number of vertices and edges on its boundary, is  $O(n)$  [KS1], [KLPS]. Since  $FP'_{\theta_i, \theta_{i+1}}$  is the free space of a rectangle, the complexity of  $FP'_{\theta_i, \theta_{i+1}}$  is also  $O(n)$ . It follows from the results in [KLPS] that  $FP_\theta$  and  $FP'_{\theta_i, \theta_{i+1}}$  can be computed in time  $O(n(\log n)^2)$  each. Also, since each  $FP_\theta$  has  $O(n)$  components,  $G'$  has  $O(l \cdot n)$  vertices. Finally, since each connected component of  $FP'_{\theta_i, \theta_{i+1}}$  is completely contained in a connected component of  $FP_\theta$  and a connected component of  $FP_{\theta_{i+1}}$ , there are at most  $O(l \cdot n)$  edges in  $G'$ . Edges between vertices in  $V_i$  and  $V_{i+1}$  can be computed in time  $O(n \log n)$  by a simultaneous plane sweep over  $FP_\theta$ ,  $FP'_{\theta_i, \theta_{i+1}}$ , and  $FP_{\theta_{i+1}}$ . So the construction of  $G'$  has time complexity  $O(l \cdot n(\log n)^2)$ .

If we preprocess each  $FP_\theta$  in time  $O(n \log n)$ , the connected components that contain the initial and final position can be computed in time  $O(\log n)$  [EGS].

Since  $|V| + |E'| = O(l \cdot n)$ , the graph exploration takes time  $O(l \cdot n)$ . Hence the running time of the restricted  $\theta$ -motion algorithm is  $O(l \cdot n(\log n)^2)$ . This proves Theorem 2.

Next we prove Theorem 3. We consider  $n$  point obstacles. Since  $\theta$ -motions arise in practice, Theorem 3 has its own merits. We use the algorithm above based on graph  $G = (\bigcup V_i, E)$  where  $u \in V_i$  and  $v \in V_{i+1}$  are connected by an edge in  $E$  iff  $C_u \cap C_v \cap FP_{\theta_i, \theta_{i+1}} \neq \emptyset$ . Note first that here  $FP_{\theta_i}$  is the complement of the union of  $n$  copies of  $R$  in orientation  $\theta_i$  placed with its centers at the obstacle points and that  $FP_{\theta_i, \theta_{i+1}}$  is the complement of the union of  $n$  copies of the rotation figure obtained by a rotation of  $R$  from orientation  $\theta_i$  to  $\theta_{i+1}$ . Since two copies of the rotation figure may intersect six times, the results in [LiS] and [KLPS] cannot be applied to determine the complexity of  $FP_{\theta_i, \theta_{i+1}}$ . We show in Section 3 that the number of vertices and edges on the boundary of  $FP_{\theta_i, \theta_{i+1}}$  is  $O(n)$ , provided that  $\theta \leq 2 \arctan(b/a)$ . This implies that each  $FP_{\theta_i, \theta_{i+1}}$  can be constructed in time  $O(n(\log n)^2)$  [KS1], [GSS]. Thus the graph  $G$  can be constructed in time  $O(l \cdot n(\log n)^2)$ . This proves Theorem 3.

**3. The Complexity of the Boundary of the Union of Simple Plane Figures.** Let  $\mathcal{F} = \{F_i; 1 \leq i \leq n\}$  be a family of  $n$  closed subsets of the plane and let  $FP = \mathbb{R}^2 - \bigcup_i F_i$  be the free space defined by  $\mathcal{F}$ . Let  $C(\mathcal{F})$  be the number of connected components of  $FP$  and let  $K(\mathcal{F})$  be the number of vertices (= intersections between boundary curves  $\text{bd}(F_i)$  and  $\text{bd}(F_j)$ ) on the boundary  $\text{bd}(FP)$  of  $FP$ . Clearly, if  $k$  is the maximal number of intersections between any two boundary curves, then  $C(\mathcal{F}) \leq K(\mathcal{F}) \leq kn^2$ . For  $k = 4$  this bound is basically the best possible as the checkerboard example of Figure 3 shows.

In [LiS] and [KLPS] it is shown that  $C(\mathcal{F}) \leq K(\mathcal{F}) \leq 6n - 12$  for  $k = 2$ . In this section we prove linear bounds for  $C(\mathcal{F})$  and  $K(\mathcal{F})$  in three cases:

- (1) If the  $F_i$ 's are wedges with the opening angle bounded from below by some constant, then  $C(\mathcal{F}) = O(n)$ .
- (2) If the  $F_i$ 's are arbitrarily stretched translational copies of some triangle  $T$  and its image  $\bar{T}$  under a halfturn, then  $C(\mathcal{F}) \leq K(\mathcal{F}) = O(n)$ .
- (3) If the  $F_i$ 's are translational copies of the rotation figure of a rectangle with sides  $a$  and  $b$ ,  $a \geq b$ , and rotation angle  $\theta \leq 2 \arctan(b/a)$ , then  $C(\mathcal{F}) \leq K(\mathcal{F}) = O(n)$ .

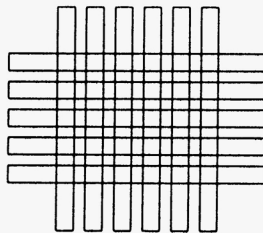


Fig. 3.

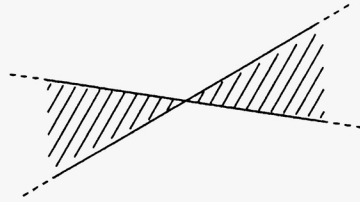


Fig. 4.

We consider double wedges first. A double wedge  $W$  is the set of all points in  $\mathbb{R}^2$  lying on different sides of two oriented straight lines  $g_1$  and  $g_2$ , i.e.,  $W = \{P \in \mathbb{R}^2 \mid P \text{ left of } g_1 \text{ and right of } g_2 \text{ or } P \text{ right of } g_1 \text{ and left of } g_2\}$  (see Figure 4). The angle between  $g_1$  and  $g_2$  is called the opening angle of  $W$ , the intersection point of  $g_1$  and  $g_2$  is called the center of  $W$ .

Consider the dualization  $\mathcal{D}_0$  that maps point  $(u, v)$  onto the straight line defined by equation  $y = ux + v$ . If the double wedge between the straight lines  $y = u_1x + v_1$  and  $y = u_2x + v_2$  does not contain a vertical line it is mapped by  $\mathcal{D}_0$  onto the line segment  $\overline{P_1P_2}$ , where  $P_i = (u_i, v_i)$ ,  $i = 1, 2$ . A double wedge containing a vertical line is mapped onto the coline segment  $g \setminus \overline{P_1P_2}$ , where  $g$  is the straight line through  $P_1$  and  $P_2$ . Clearly, a point  $P$  lies in the complement of a double wedge  $W$  iff the line  $\mathcal{D}_0(P)$  dual to point  $P$  does not intersect the (co-)line segment  $\mathcal{D}_0(W)$ . Parallel lines are assumed to intersect at infinity. The two connected components of the complement of  $W$  are mapped into the set of nonvertical lines lying above and below  $\mathcal{D}_0(h)$ , respectively, and not intersecting  $\mathcal{D}_0(W)$  where  $h$  is some fixed straight line contained in  $W$ .

Now consider the complement of the union of  $n$  double wedges. Two points  $Q_1$  and  $Q_2$  lie in the same connected component of free space iff there is a path connecting  $Q_1$  and  $Q_2$  avoiding the double wedges. This is the case iff  $\mathcal{D}_0(Q_1)$  can be translated and rotated onto  $\mathcal{D}_0(Q_2)$  without collision with the (co-)line segments dual to the double wedges. The motion of  $\mathcal{D}_0(Q_1)$  must also avoid vertical positions (which are dual to points at infinity). In this case we call  $\mathcal{D}_0(Q_1)$  and  $\mathcal{D}_0(Q_2)$  *topologically equivalent*. In this way we partition the set of nonvertical lines which do not intersect (co-)line segments dual to the wedges into *topological equivalence classes*.

LEMMA 3.1. *Let  $\mathcal{W} = \{W_1, \dots, W_n\}$  be a set of translational copies of a double wedge. Then  $C(\mathcal{W}) = O(n)$ .*

PROOF. We may assume without loss of generality that the double wedges do not contain a vertical line. The endpoints of the line segments dual to the wedges lie on two vertical lines (see Figure 5), because the  $x$ -coordinates of them are determined by the slopes of the lines bounding the wedges. It is easy to see that the number of topological equivalence classes of lines with respect to the straight line segments dual to the double wedges is  $O(n)$  and hence  $C(\mathcal{W}) = O(n)$ . □



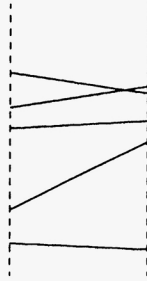


Fig. 5.

If rotational copies are allowed, the number of connected components may be as large as  $n^2$  because the checkerboard construction is possible again. However if we bound the opening angle from below the number of connected components is linear.

LEMMA 3.2. *Let  $\mathcal{W} = \{W_1, \dots, W_n\}$  be a set of double wedges with the opening angle greater than some constant  $\alpha_0$ . Then  $C(\mathcal{W}) = O(n)$ .*

PROOF. Again we use dualization  $\mathcal{D}_0$  and count the number of topological equivalence classes of lines with respect to the (co-)line segments  $l_1, \dots, l_n$  dual to  $W_1, \dots, W_n$ . The requirement on the opening angle implies

OBSERVATION 3.1. There are constants  $d$  and  $e$  such that for each double wedge  $W_i$  either the dual of  $W_i$  is a line segment of horizontal length greater than  $d$  or the dual of  $W_i$  is a coline segment and the  $x$ -coordinate of one of its endpoints has absolute value less than  $e$ .

Next observe that all topological equivalence classes remain if we shorten some of the line segments. The topological equivalence classes may become larger and new classes may appear because of lines that do not cut the shortened segment any more but did before. Hence we have

OBSERVATION 3.2. Suppose some line segment  $l_k$  is shortened to a line segment  $l'_k \neq \emptyset$ ,  $l'_k \subset l_k$ . Then the number of topological equivalence classes does not decrease.

Since lines in the different topological equivalence classes with respect to a coline segment cannot be moved onto each other without going through a vertical position, even if we omit one ray of the coline segment, we have further

OBSERVATION 3.3. Suppose one ray of some coline segment  $l_k$  is omitted. Then the number of topological equivalence classes does not decrease.

Using observations 3.1–3.3 we now show that the number of equivalence classes with respect to  $L = \{l_1, \dots, l_n\}$  is  $O(n)$ . From each coline segment in  $L$  we omit one ray such that the remaining one has its  $x$ -coordinate in  $[-e, e]$ .

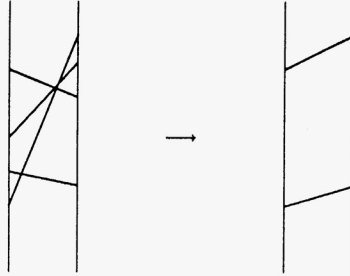


Fig. 6.

Now starting from the  $x$ -value  $-e - d/2$  we decompose the plane into vertical stripes of width  $d/2$  up to the  $x$ -value  $e + d/2$ . By Observation 3.1 it is clear that each segment  $l_i$  traverses at least one stripe  $s$  completely. We cut from  $l_i$  the parts outside of  $s$ . So we have left a set of line segments each ending at the left and right boundary of some stripe. We obtain a set of constantly (depending on  $\alpha_0$ ) many stripes. Let  $L'$  be the set of line segments constructed this way. By Observations 3.2 and 3.3 the number of topological equivalence classes with respect to  $L'$  is an upper bound for the number of topological equivalence classes with respect to  $L$ .

To bound the number of topological equivalence classes with respect to  $L'$  we first bound the number of topological equivalence classes with respect to line segments in only two vertical stripes and then extend this to the constantly many stripes containing the lines in  $L'$ . Consider the case that we have a left stripe and a right stripe of width 1 each and distance  $f$  between them. Let  $n_l$  ( $n_r$ ) be the number of line segments in the left (right) stripe and let  $m = n_l + n_r$ . We first replace connected sets of intersecting line segments by the two line segments between the highest left and highest right endpoints and between the lowest ones (see Figure 6), thereby clearly not decreasing the number of topological equivalence classes.

Now the line segments divide the stripes into (bounded and unbounded) trapezoids. We say that a line  $g$  leads through a trapezoid  $T$  if  $g$  intersects  $T$  but misses the line segments bounding  $T$  from above and below. In order to count the number of topological equivalence classes whose lines lead through bounded trapezoids, we represent each bounded trapezoid by a node in an undirected bipartite graph  $G_w = (V_l \cup V_r, E)$ , where  $V_l$  ( $V_r$ ) are the nodes (bounded trapezoids) in the left (right) stripe. There are  $m - 2$  bounded and 4 unbounded trapezoids provided that  $n_l, n_r \geq 1$ . There is an edge between two nodes if a straight line exists that leads through the corresponding bounded trapezoids. Each trapezoid  $T_r$  in the right stripe that is connected to a trapezoid  $T_l$  by an edge of  $G_w$  must intersect the trapezoid  $T_{l,max}$  defined by the right stripe and the lines leading through  $T_l$  with minimal and maximal slope (see Figure 7). At most two trapezoids in the right stripe connected to  $T_l$  in  $G_w$  are not completely contained in  $T_{l,max}$ .

Some calculation shows that the sum of the lengths of the left and the right side of  $T_{l,max}$  is at most  $(2f + 3)$  times the sum of the lengths of the left and

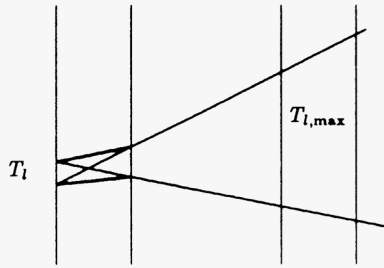


Fig. 7.

the right side of  $T_l$ . We associate with each node  $u$  the sum of the lengths of the left and right sides of the corresponding trapezoid as its weight  $w(u)$ . For each node  $u$  in  $V_l$  we delete the edges connecting  $u$  to the nodes in  $V_r$  that represent the trapezoids that are not completely contained in  $T_{l,max}$ . The same is done for each node in  $V_r$ . Note that the number of deleted edges is at most  $2(m - 2)$ . Then

$$(*) \quad \sum_{\{u, v\} \in E} w(v) \leq (2f + 3)w(u)$$

for all nodes  $u \in V_l \cup V_r$ . Consider the node with smallest weight. It has at most  $2f + 3$  neighbors. After deletion of this node and all incident edges property (\*) still holds. It follows that  $G_w$  has at most  $(2f + 5)(m - 2)$  edges. Since there are at most  $2m$  topological equivalence classes whose lines lead through at least one unbounded trapezoid, the overall number of topological equivalence classes is  $O(fm)$ .

We use this result to derive a bound on the number of topological equivalence classes with respect to the lines in  $L'$ . The lines in  $L'$  are distributed over  $k$  stripes with width  $d/2$ , where  $k = 2(\lambda e + d)/d$ . The maximal distance between two stripes is  $2e$ . The above result implies that the number of topological equivalence classes is at most  $cn$  for some constant  $c$  depending on  $\alpha_0$  if we consider only the line segments in any two of the  $k$  stripes. For each topological equivalence class with respect to  $L'$  we choose a sample line and a sample point on it. We rotate this sample line counterclockwise around the sample point as far as possible until one of the line segments in  $L'$  is touched. Next we rotate counterclockwise around the touching point until another line segment is touched. If the sample line happens to be flush with the line segment before touching any other line segment we continue rotating about the other endpoint. Now each sample line touches at least two line segments. We assign each topological equivalence class of  $L'$  to the pair of stripes in which the line segments touched by the corresponding sample line lie. Observe that for each pair of stripes this defines an injective mapping from the set of topological equivalence classes with respect to  $L'$  assigned to this pair into the set of topological equivalence classes with respect to the line segments in these stripes. Hence the number of topological equivalence classes of  $L'$  is at most  $k^2 cn$  for constants  $k$  and  $c$  depending on  $\alpha_0$ . Thus  $C(\mathcal{W}) = O(n)$ .  $\square$

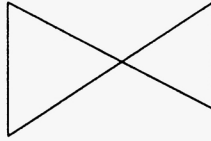


Fig. 8.

In our next step toward the rotation body of a rectangle we consider double wedges bounded by vertical lines from left and right (see Figure 8). In fact, we consider a more general problem.

LEMMA 3.3. *Let  $T$  be an arbitrary triangle and let  $\bar{T}$  be the image of  $T$  under a halfturn. Let  $\mathcal{T} = \{T_1, \dots, T_n\}$ , where  $T_i = a_i + \alpha_i T$  or  $T_i = a_i + \alpha_i \bar{T}$  for some  $a_i \in \mathbb{R}^2$ ,  $\alpha_i \in \mathbb{R}$  and  $a_i + \alpha T = \{a_i + (\alpha x, \alpha y); (x, y) \in T\}$ . Then  $K\mathcal{T} = O(n)$ .*

PROOF. We classify the corners on the boundary of free space into three types. Corners of a triangle are of type A. We say that triangles  $T_i$  and  $T_j$  have the same orientation if both are copies either of  $T$  or  $\bar{T}$ . Intersection points of edges of triangles of the same orientation are type B corners. Intersection points of edges of triangles of different orientation are type C corners. Clearly, the number of type A corners is at most  $3n$ . Next observe that the boundaries of two triangles of the same orientation intersect only twice. Thus it follows from the results in [KLPS] that the number of corners of type B is at most  $6n - 12$ . We call all corners of type A and B countable. The boundaries of two triangles in different orientation may intersect in six points. Hence the results in [KLPS] cannot be applied. A corner  $c$  of type C is called countable if for at least one of the intersecting edges it is the leftmost or rightmost intersection point on that edge lying on the boundary of free space, i.e., there is no other corner on the boundary lying between one of the endpoints of the edge and corner  $c$ . We assign  $c$  to this endpoint. There are at most  $6n$  countable type C corners.

Assume there is a corner  $c_1$  of type C that is not countable. Let  $T_1$  and  $T_2$  be the intersecting triangles and let  $e_1$  and  $e_2$  be the intersecting edges. Start in  $c_1$  and walk along the edge  $e_2$  of  $T_2$  on the boundary of free space (see Figure 9).

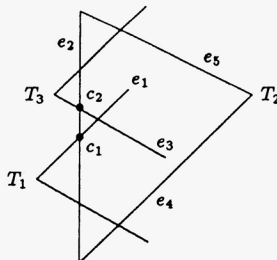


Fig. 9.

Let the next corner  $c_2$  met be the intersection of edge  $e_3$  of triangle  $T_3$  and  $e_2$ . Assume that  $c_2$  is not countable. Let  $e_4$  and  $e_5$  be the other two edges of  $T_2$  where on a traversal of  $e_2$  starting in the common endpoint of  $e_2$  and  $e_4$  we first encounter  $c_1$  and then  $c_2$ . Since we have assumed that the right endpoint of  $e_1$  is not covered by  $T_2$ , line segment  $e_1$  must intersect  $e_5$  (note that  $e_1 \parallel e_4$ ). By the same reason  $e_3$  has to intersect  $e_4$ . Hence  $e_1$  and  $e_3$  intersect. However,  $T_1$  and  $T_3$  have the same orientation, so the right endpoint of  $e_1$  is covered by  $T_3$  or the right endpoint of  $e_3$  is covered by  $T_1$ , a contradiction to the fact that both  $c_1$  and  $c_2$  are not countable. It follows that the number of type C corners on the boundary of the complement of the union of the  $n$  triangles that are not countable is not larger than the number of countable corners on the boundary. Thus  $K(\mathcal{T}) = O(n)$ .  $\square$

Now we are ready to consider bow ties.

LEMMA 3.4. *Let  $\mathcal{B} = \{B_1, \dots, B_n\}$  be a set of translational copies of the rotation figure of a rectangle with sides  $a \geq b$ , where the rotation angle is a fixed angle of size  $2 \arctan(b/a)$  at most. Then  $K(\mathcal{B}) = O(n)$ .*

PROOF. Since the boundaries of two translational copies of a bow tie may have six intersection points the result in [KLPS] cannot be applied here. We subdivide the boundary of the rotation figure in segments (straight line segments and arcs) as shown in Figure 10.

For each pair of segment types we show that the number of intersection points lying on  $\text{bd}(\bigcup_{i=1}^n B_i)$  is linear. Table 1 contains all cases together with a hint on the counting argument that is used to show the linearity.

The entries in the table have the following meaning. Entry  $C$  means that there is a convex subset of the rotation figure containing both segments in its boundary. It is known that the complexity of the union of translational copies of a convex set is linear [KLPS]. Since intersection points between the corresponding segments are also on the boundary of the union of the convex subsets, the number of such intersection points on  $\text{bd}(\bigcup B_i)$  is  $O(n)$ .

In all cases with entry  $\Delta$  Lemma 3.3 can be applied. We expand each segment to a triangle that is completely contained in the rotation figure such that the triangle containing the first segment is the image of the triangle of the second segment under a halfturn (see, for example, Figure 11).

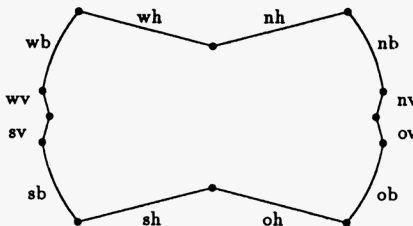


Fig. 10.

Table 1.

	sv	sb	sh	oh	ob	ov	nv	nb	nh	wh	wb	wv
sv	C	C	C	C	C	C	C	C	C	C	—	Δ
sb	C	C	C		0	C	C	C	C	C	0	
sh	C	C	C	Δ	—	C	C	C	C	C	C	C
oh	C	—	Δ	C	C	C	C	C	C	C	C	C
ob	C	0		C	C	C		0	C	C	C	C
ov	C	C	C	C	C	C	Δ	—	C	C	C	C
nv	C	C	C	C	—	Δ	C	C	C	C	C	C
nb	C	C	C	C	0		C	C	C		0	C
nh	C	C	C	C	C	C	C	C	C	Δ	—	C
wh	C	C	C	C	C	C	C	—	Δ	C	C	C
wb		0	C	C	C	C	C	0		C	C	C
wv	Δ	—	C	C	C	C	C	C	C	C	C	C

Since all intersection points of the segments on  $\text{bd}(\cup B_i)$  are also on the boundary of the union of these triangles there are  $O(n)$  such points by Lemma 3.3.

We next turn to the entries marked — and |. Each entry marked — has the following property: All other entries in that row are marked C or Δ and the entry corresponds to an intersection of a straight line segment and an arc, no two of which can be contiguous on the boundary of free space. Hence the number of intersections corresponding to all — entries is bounded by the number of intersections with C and Δ entries plus the number of segments. The argument for | entries is analogous; we only have to replace row by column in the argument above.

We are left with the entries marked 0. In these cases we can show that at least one of the endpoints of the intersecting arcs is covered by the other rotation figure, such that the part of the arc between the intersection point and the endpoint lies in the interior of the union of the rotation figures. As in the proof of Lemma 3.3 we assign the intersection point to the covered endpoint. It is clear that each endpoint of an arc gets at most one attributed intersection point. Let us, for example, consider an intersection point between an nb-arc  $a_i$  of  $B_i$  and an ob-arc  $a_j$  of  $B_j$ . Let  $R_k$  denote the upper endpoint of arc nb in  $B_k$  and  $T_k$  the lower endpoint. Furthermore, let  $U_k$  denote the upper endpoint of arc ob in  $B_k$  and  $S_k$  the lower endpoint,  $k = i, j$  (see Figure 12).

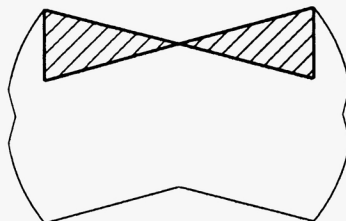


Fig. 11.

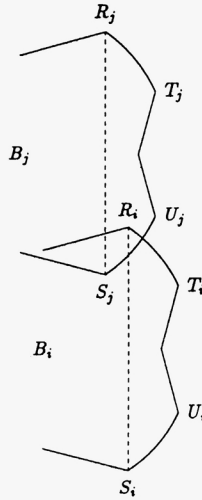


Fig. 12.

We now distinguish cases. Either  $R_i$  lies on or to the right of  $R_jS_j$  or  $S_j$  lies to the right of  $R_iS_i$ . In the former case,  $R_i$  lies to the left of line segment  $U_jR_j$  and above arc  $a_j$  and hence  $R_i$  is contained in bow tie  $B_j$ . In the latter case,  $S_j$  is covered by  $B_i$  by the symmetric argument. This proves that the number of  $(nb, ob)$ -intersections is linear. Similar arguments can be used for all type  $\theta$  entries. This completes the proof of Lemma 3.4.  $\square$

**4. Conclusions.** We have introduced the tightness  $\varepsilon_{\text{crit}}$  of the motion planning problem for a rectangle and have shown that the motion of a rectangle can be planned in time  $O(((a/b)(1/\varepsilon_{\text{crit}}) + 1)n(\log n)^2)$ , where  $n$  is the size of the polygonal environment. We have also shown how to plan  $\theta$ -motions in time  $O((1/\theta) \cdot n(\log n)^2)$ . The latter result is based on the fact that the complexity of the boundary of the union of  $n$  bow ties is  $O(n)$ . We believe that similar results can be obtained for more general motion planning problems.

## References

- [CK] L. P. Chew and K. Kedem, High-Clearance Motion Planning for a Convex Polygon among Polygonal Obstacles, Technical Report No. 184/90, Tel Aviv University (1990).
- [EGS] H. Edelsbrunner, L. Guibas, and J. Stolfi, Optimal Point Location in a Monotone Subdivision, *SIAM J. Comput.* **15** (1986), 317–340.
- [GSS] L. Guibas, M. Sharir, and S. Sifrony, On the General Motion Planning Problem with Two Degrees of Freedom, *Discrete Comput. Geom.* **4** (1988), 491–521.
- [KLPS] K. Kedem, R. Livne, J. Pach, and M. Sharir, On the Union of Jordan Regions and Collision-free Motion Amidst Polygonal Obstacles, *Discrete Comput. Geom.* **1** (1986), 59–71.

- [KS1] K. Kedem and M. Sharir, An Efficient Algorithm for Planning Collision-free Translational Motion of a Convex Polygonal Object in 2-dimensional Space Amidst Polygonal Obstacles, *Proc. First ACM Symp. on Computational Geometry*, 1985, pp. 75–80.
- [KS2] K. Kedem and M. Sharir, An Efficient Motion-Planning Algorithm for a Convex Polygonal Object in Two-Dimensional Polygonal Space, *Discrete Comput. Geom.* **5** (1990), 43–75.
- [LeS] D. Leven and M. Sharir, Planning a Purely Translational Motion for a Convex Object in Two-Dimensional Space Using Generalized Voronoi Diagrams, *Discrete Comput. Geom.* **2** (1987), 9–31.
- [LiS] R. Livne and M. Sharir, On Intersection of Planar Jordan Curves, Technical Report No. 153, Robotics Report No. 37, Courant Institute, New York (1985).
- [LPW] T. Lozano-Perez and M. Wesley, An Algorithm for Planning Collision-free Paths Among Polyhedral Obstacles, *Comm. Assoc. Comput. Mach.* **22** (1979), 560–570.
- [S] M. Sharir, Davenport–Schinzel Sequences and Their Geometric Applications, *Theoretical Foundations of Computer Graphics and CAD* (edited by R. A. Earnshaw), Springer-Verlag, Berlin, 1988, pp. 253–272.